

Journal of Materials Chemistry C

Accepted Manuscript



This is an *Accepted Manuscript*, which has been through the Royal Society of Chemistry peer review process and has been accepted for publication.

Accepted Manuscripts are published online shortly after acceptance, before technical editing, formatting and proof reading. Using this free service, authors can make their results available to the community, in citable form, before we publish the edited article. We will replace this *Accepted Manuscript* with the edited and formatted *Advance Article* as soon as it is available.

You can find more information about *Accepted Manuscripts* in the [Information for Authors](#).

Please note that technical editing may introduce minor changes to the text and/or graphics, which may alter content. The journal's standard [Terms & Conditions](#) and the [Ethical guidelines](#) still apply. In no event shall the Royal Society of Chemistry be held responsible for any errors or omissions in this *Accepted Manuscript* or any consequences arising from the use of any information it contains.

Cite this: DOI: 10.1039/c0xx00000x

PAPER

www.rsc.org/xxxxxx

A Novel Intermediate Connector with Improved Charge Generation and Separation for Large-Area Tandem White Organic Lighting Devices

Lei Ding, Yan-Qiu Sun, Hua Chen, Feng-Shuo Zu, Zhao-Kui Wang*, and Liang-Sheng Liao*

Received (in XXX, XXX) XthXXXXXXXXXX 20XX, Accepted Xth XXXXXXXXXXXX 20XX

DOI: 10.1039/b000000x

An intermediate connector (IC) consisting of lithium (Li) doped 4,7-diphenyl-1,10-phenanthroline (BPhen)/Al/tetrafluoro-tetracyanoquinodimethane (F₄-TCNQ)/1,4,5,8,9,11-hexaazatriphenylene-hexacarbonitrile (HAT-CN) is developed for fabricating tandem white organic light-emitting diodes (WOLEDs). The investigation of charge generation and separation process in Bphen: Li/Al/F₄-TCNQ/HAT-CN, which is carried out by the analysis of current-voltage and capacitance-voltage characteristics, shows that the proposed IC structure is suitable as a connecting unit in tandem OLEDs. The tandem WOLED based on a silicon compound host material of 10-phenyl-2'-(triphenylsilyl)-10H-spiro [acridine-9,9'-fluorene] (SSTF) with proposed IC structure exhibits a maximum current efficiency of 159.2 cd A⁻¹ and a maximum power efficiency of 69.4 lm W⁻¹, respectively. For application in large-area OLEDs, a 150 × 150 mm² tandem lighting panel with maximum efficiencies of 231.8 cd A⁻¹ and 52.9 lm W⁻¹, correlated color temperature of 3000 K and Commission International de l'Eclairage (CIE) coordinates of (0.34, 0.45) is also demonstrated.

Introduction

Organic light-emitting diodes (OLEDs) have drawn considerable attention as the solid state lighting owing to its human-friendly characteristics and great potential of becoming a high-performance light source in the future. However, efficiency, lifetime and panel size are still the main issues for their practical applications.¹⁻³ Presently, white phosphorescent OLEDs have demonstrated comparable efficiency and lifetime with conventional lighting such as tungsten light bulb, halogen lamp, or even fluorescent lamp.^{4,5} Noticeably, the high efficiency of most reported white OLEDs are achieved in small emitting area (e.g., 3 × 3 mm²).⁶ When the OLED is operated at a large brightness over 3000 cd m⁻² continuously, the driving voltage is increased gradually, resulting in a lowered power efficiency. This situation becomes worse for the large size panels.⁷ Therefore, the larger the emitting area, the worse the OLED performance.⁸

Institute of Functional Nano & Soft Materials (FUNSOM), Soochow University, Suzhou, Jiangsu 215123, China.

Email: zkwang@suda.edu.cn; lsiao@suda.edu.cn.

Fax: +86-65882846. Tel: +86-512-65880945

†Electronic Supplementary Information (ESI) available. See DOI: 10.1039/b000000x/

It is then a desire to fabricate a large area OLED that can be operated at high brightness without reducing device performance.⁹

OLED lighting panels are generally fabricated by using a tandem structure, in which all of the emitting layer (EL) units are electrically connected in series by inserting an intermediate connector (IC) between adjacent EL units.¹⁰ IC in the tandem OLEDs consists of an electron accepting layer and an electron donating layer.¹¹ At applied voltages, electrons in the highest occupied molecular orbital (HOMO) of the electron donating material are injected into the lowest unoccupied molecular orbital (LUMO) of the electron accepting material, leading to the generation of electrons in the accepting layer and holes in the donating layer, followed by the charge separation process.¹² Three types of IC structures including: organic/metal oxide,¹³⁻¹⁸ bulk heterojunction,^{19,20} and organic/organicheterojunction²¹⁻²⁴ have been developed in tandem OLEDs. However, some of tandem OLEDs show higher driving voltage than that of the conventional device because of additional barrier caused by the intermediate connector.

In this paper, we proposed a novel IC with a structure of lithium (Li) with 4,7-diphenyl-1,10-phenanthroline (BPhen)/Al/tetrafluoro-tetracyanoquinodimethane (F₄-TCNQ)/1,4,5,8,9,11-hexaazatriphenylene-hexacarbonitrile (HAT-CN) for fabricating tandem white OLEDs. Li can act as an n-dopant which comes from the decomposition of LiH during the evaporation owing to the advantages of easy evaporation and simple decomposition

reaction of LiH. F₄-TCNQ was inserted between Bphen: Li/Al and HAT-CN for aligning the energy levels of *n*-type and *p*-type layers. As a result, the fabricated blue/yellow phosphorescent white OLEDs using Bphen: Li/Al/F₄-TCNQ/HAT-CN as the IC demonstrated a maximum current efficiency of 159.2 cd A⁻¹ and power efficiency of 69.4 lm W⁻¹, respectively, without any outcoupling technology. Meanwhile, a 150 × 150 mm² white OLED panel based on same tandem structure exhibited a maximum current efficiency of 231.8 cd A⁻¹ and a maximum power efficiency of 52.9 lm W⁻¹ by a diffuser film.

Experimental

OLEDs were fabricated on the cleaned glass substrates pre-coated with 110 nm ITO (15Ω □⁻¹), after a 15 min UV ozone treatment. All layers were deposited by thermal evaporation under a base vacuum of about 10⁻⁶ torr. The other organic materials and metal were evaporated in the rate of 3-5 Å s⁻¹ and 8-10 Å s⁻¹, respectively. The tandem white OLEDs were fabricated using all phosphorescent white-emitting units 10-phenyl-2'-(triphenylsilyl)-10H-spiro [acridine-9,9'-fluorene (SSTF): bis (4,6-difluorophenylpyridinato-N,C2') picolinate (Flrpic)/SSTF: Iridium (III) bis(4-phenylthieno [3,2-c] pyridinato-N,C2') (PO-01), which were connected with an ICs structure of Bphen: Li/Al/F₄-TCNQ / HAT-CN. SSTF was used as a host in both blue and yellow emitting layers. Flrpic and PO-01 were used as the blue and the yellow dopant, respectively. 1,3,5-Triazo-2,4,6-triphosphorine-2,2,4,4,6,6-tetrachloride (TAPC) was used as the hole transport layer (HTL), 1,3,5-tri(m-pyrid-3-yl-phenyl) benzene (TmPyPB) was used as electron transport layer (ETL). The diffuser film comprising TiO₂ particles was formed on the glass substrate surface by spin-coating a kind of TiO₂ matrix at 2500 rpm. To make the kind of matrix with well-dispersed TiO₂ particles, we synthesized TiO₂ sol by sol-gel method.

The luminance, electroluminescent (EL) spectra and the Commission International de l'Eclairage (CIE) coordinates of all devices were measured by using a PR-655 photometer. Current density-voltage (*J-V*) measurements were carried out using a Keithley 2400 Source Meter. The emitting area of the white OLED devices and lighting panel are 3 × 3 mm² and 150 × 150 mm², respectively. The Ultraviolet photoelectron spectroscopy (UPS) was carried out to evaluate the energy levels of Li doped and non-doped Bphen films. The capacitance-voltage characteristics were analyzed using a Keithley 4200 semiconductor characterization system. UV/Vis spectrophotometer (PerkinElmer Lambda 750) was used to measure the transmittance of intermediate layer.

Results and Discussion

Intermediate Connector

Characteristics of Intermediate Connector

The IC consists of in sequence Bphen: Li (1.2 vol%, 55 nm), Al (0.5 nm), F₄-TCNQ (1 nm) and HAT-CN (10 nm). The *n*-type layer (Bphen: Li) is placed adjacent to the ETL of an organic EL unit towards the anode side, and the F₄-TCNQ/HAT-CN bilayer is located adjacent to the HTL of the second organic EL unit

towards the cathode side. The Al thin film in the intermediate connectors is to further improve the carrier injection, acting as a *n*-type deep doping or a trap center. In addition, in some extent, it also has a role in preventing the interdiffusion or interaction between the *n*-type doped EIL in the preceding EL unit and the *p*-type doped HIL of the adjacent EL unit to stabilize the driving voltage during operation. In addition, the polarized optical microscopic evaluations demonstrated that a doping of Li into Bphen can solve the issues of instability and crystallization of Bphen film^{25,26} which is beneficial for the lifetime of tandem OLEDs. Figure 1 shows the Polarized optical microscope images of the thin films (I)-(IV) for pristine Bphen and (V)-(VIII) for Bphen: Li for 0, 15, 30, 45 min in air, respectively. The two samples were fabricated at the same time.

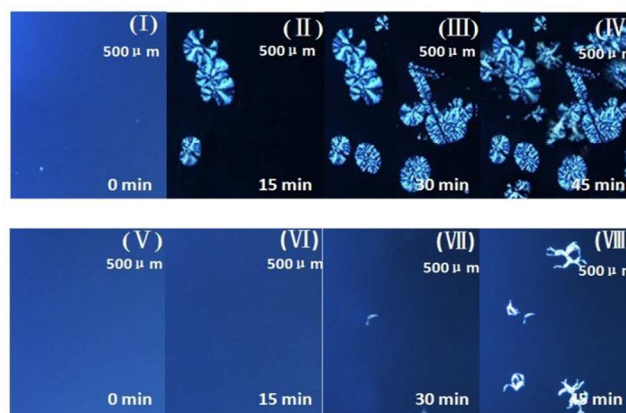


Fig 1. Polarized optical microscope images of the thin films (I)-(IV) for pristine Bphen and (V)-(VIII) for Bphen: Li for 0, 15, 30, 45 min in air, respectively.

UPS and XPS spectra of Li doped Bphen films are measured in order to better understand the function of Bphen: Li in the tandem OLEDs. Figure 2a shows the UPS spectra for the secondary electron cutoff region and the HOMO region of Bphen and Bphen: Li (1.2 vol%) films. From the UPS spectra, the HOMO level relative to the Fermi level is 3.0 eV and 3.5 eV, respectively, for pristine and Li-doped Bphen, which can be obtained by extrapolating in the valence band region. The vacuum level (3.38 eV and 2.95 eV for Bphen and Li-doped Bphen, respectively) can also be calculated according to the secondary electron cut off region. As a consequence, the HOMO level with respect to the vacuum level (ionization potential) is about 6.38 eV and 6.45 eV. It suggests that the Fermi level (*E_F*) moves towards the lowest unoccupied molecular orbitals (LUMO), which means the electron injection barrier between the LUMO and Fermi level offset was dramatically decreased. Figure 2b shows the XPS spectra of the Bphen and Bphen: Li (1.2 vol%) films. In Li-doped Bphen film, the peaks of N1s shift to lower binding energy, indicating a transfer process of electrons from Li to Bphen. Meanwhile, the shift of Fermi levels due to doping effect will result in a nearly ohmic contact at the interface, which will greatly improve the charge carrier injection.²⁷

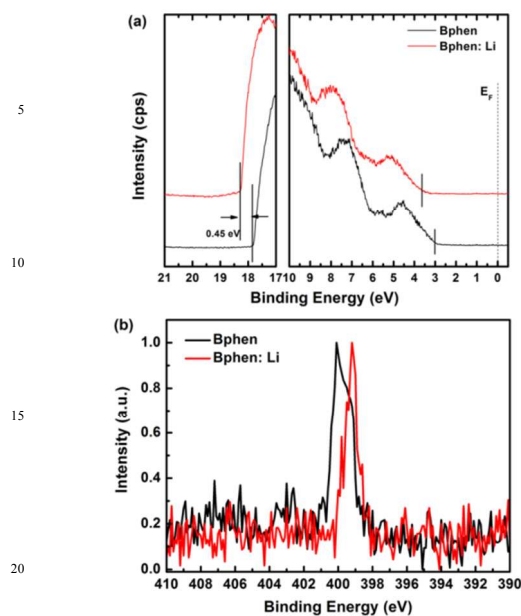


Fig 2. (a) The UPS spectra for the secondary electron cutoff region and the HOMO region of the Bphen and Bphen: Li films, (b) The XPS spectra from N1s core level for undoped and Li doped Bphen film.

Figure 3 shows the transmittance of the intermediate connector layer Bphen: Li (1.2 vol%, 55 nm), Al (0.5 nm), F₄-TCNQ (1 nm) and HAT-CN (10 nm). The whole IC exhibits a high transmittance of 90%-94% in the wavelength range of 380-780 nm, which is transparent enough for tandem white OLEDs.

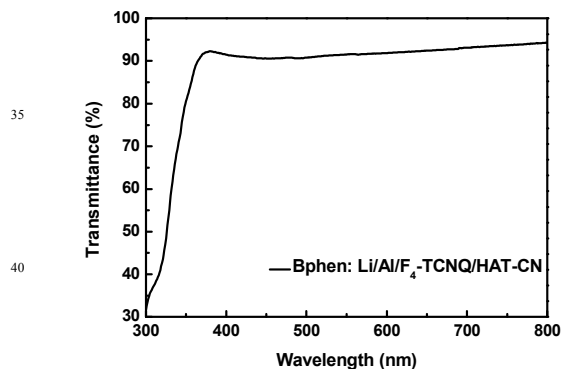


Fig 3. Transmittance spectra of Bphen: Li/Al/F₄-TCNQ/HAT-CN.

Charge Separation and Transportation Mechanism of ICs

In order to investigate the function of IC in tandem OLEDs, hole-only light emitting devices with different ICs are fabricated as: ITO/NPB (75nm)/Alq₃ (60nm)/IC/NPB (50nm)/Al (150nm), where "IC" stands for Bphen: Li/Al (Device A-1), F₄-TCNQ/HAT-CN (Device A-2), Bphen: Li/Al/HAT-CN (Device A-3), Bphen: Li/Al/F₄-TCNQ/HAT-CN (Device A-4), respectively. Figure 4 shows the energy diagram of the hole-only light-emitting device consisting of *n*-type layer Bphen: Li/Al and *p*-type bilayers F₄-TCNQ/HAT-CN. The large energy barrier at NPB/Alq₃ interface can effectively prevent the electron inject into NPB layer from Alq₃, while the IC can generate and separate charge carriers into the adjacent layer. Therefore, holes from ITO

and electrons from IC can be well confined within the interface between NPB and Alq₃. In addition, the energy alignment by IC can lead to efficient electron transfer from the HOMO of NPB to the LUMO of HAT-CN upon a certain electric field.

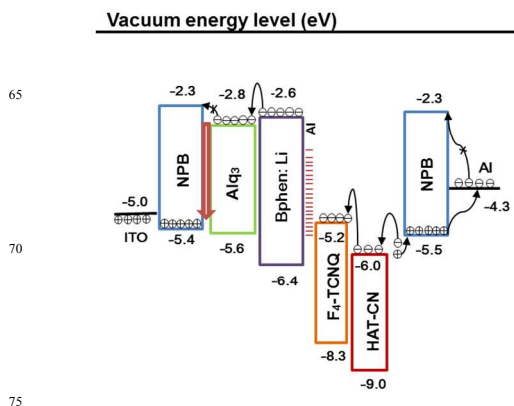


Fig 4. Schematic energy level diagram of the IC used in the hole-only light-emitting device.

Figure 5 shows the *J-V* and *J-L* characteristics of the hole-only light emitting devices with various ICs. Device A-1 shows extremely low current density without any luminance. It means that no electrons are generated in the IC of Bphen: Li/Al and/or corresponding interfaces. The luminance is still not yet observed in device A-2 although the current density is obviously enhanced. At the interface of Alq₃/F₄-TCNQ, electron at the HOMO (-5.6 eV) of Alq₃ can easily transfer to the LUMO (-5.2 eV) of F₄-TCNQ due to a low energy barrier between them. Under forward bias, holes inject into the adjacent HAT-CN layer and transport to the NPB layer toward the Al cathode. Nevertheless, electrons can not inject into the Alq₃ layer due to the large energy barrier between them. Therefore, no light emission was observed in the device A-2. Device A-3 and A-4 exhibit obvious Alq₃ emission. When F₄-TCNQ/HAT-CN is added, electrons are extracted from the LUMO of HAT-CN into the LUMO of F₄-TCNQ, and then jump on the LUMO of Bphen: Li since the electron barrier is decreased by the Li doping effect. In all, the increase of current density is obvious in whole voltage range when adding the HAT-CN layer. Particularly, comparing with the case of only using the HAT-CN layer, there is also obvious increase of current density in lower voltage (< 4 V) in the case of using both F₄-TCNQ/HAT-CN layers. We attributed it to the formation of an efficient gradient barrier in the IC after adding the F₄-TCNQ/HAT-CN layers, making the charge carrier transfer easily in the IC.

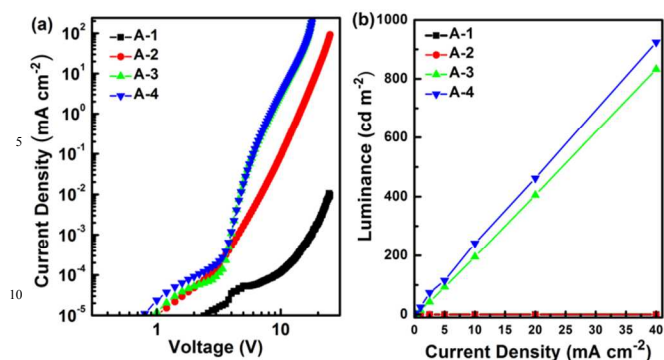


Fig 5. Voltage vs. current density (a) and luminance vs. current density (b) characteristics of the hole-only device with different ICs.

To investigate the function of the IC of Bphen: Li/Al/F₄-TCNQ/HAT-CN on the charge separation process, two devices were fabricated with structures of ITO/Bphen (50 nm)/(with and without (W/O)), IC (Bphen: Li/Al/F₄-TCNQ/HAT-CN)/NPB (50 nm)/Al. The capacitance-voltage characteristics were analyzed using a Keithley 4200 semiconductor characterization system. As shown in Figure 6, almost no changes in capacitance with the applied voltages from -6 V to 6 V are observed in the device without IC. The Bphen and NPB layer can effectively prevent charge carrier injection from corresponding electrodes since the large barriers existed at the interfaces of ITO/Bphen and NPB/Al. It indicates that no charge was generated in the interface of Bphen/NPB. However, the capacitance in the device with IC device was almost constant until 3.4 V, then sharply increased with a maximum peak at 6 V. That's because the holes and electrons were generated and injected into the adjacent NPB and Bphen layer, respectively. After that the capacitance dropped rapidly with further increase of external voltage because the charge carriers begin to transport to the counter electrodes. It suggests that the IC layers of Bphen: Li/Al/F₄-TCNQ/HAT-CN plays an important role in the charge separation process.

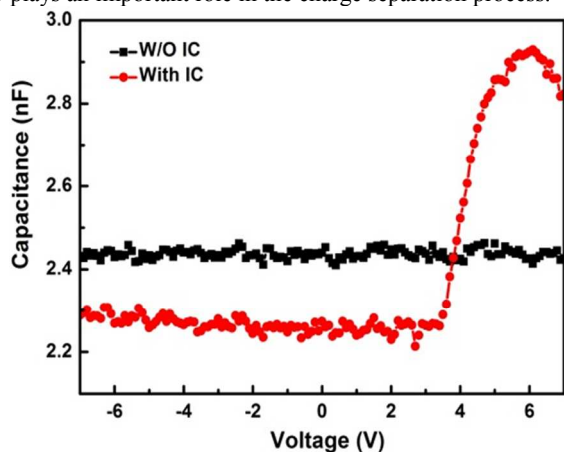


Fig 6. Capacitance-voltage characteristics of ITO/Bphen (50 nm)/(with and without IC (Bphen: Li/Al/F₄-TCNQ/HAT-CN)/NPB (50 nm)/Al.

High Efficiency WOLEDs

Novel Host Material for WOLEDs

Spiro structure based SSTF is a novel silicon-based compound with a triplet energy of 2.81 eV and a glass transition temperatures of 109 °C, which are comparable with traditional host materials.²⁸ SSTF host based on phosphorescent white OLED (emitting area: 3 × 3 mm²) with a structure of ITO/HAT-CN (10 nm)/TAPC (45 nm)/SSTF: Flrpic 15 vol% (19 nm)/SSTF: PO-01 9 vol% (1 nm)/TmPyPB (40 nm)/Liq (2 nm)/Al was fabricated. For comparison, mCP and TPBi based reference device with a structure of ITO/HAT-CN (10 nm)/TAPC (45 nm)/mCP: Flrpic 15 vol% (19 nm)/TPBi: PO-01 9 vol% (1 nm)/TmPyPB (40 nm)/Liq (2 nm)/Al was also fabricated. Figure 7a. shows the current density-luminance-voltage (*J-L-V*) characteristics of two WOLEDs. In SSTF host based device, the current density and luminance obviously increased with reduced driving voltage compared with the reference device. The increased luminance and the reduced driving voltage is attributed to the efficient carrier injection and transport in SSTF host based device owing to high hole mobility and wide triplet energy of SSTF. Figure 7b shows the current and power efficiency as a function of luminance in two devices. The SSTF host based device demonstrated a current efficiency of 65 cd A⁻¹ and a power efficiency of 52.3 lm W⁻¹ at 1000 cd m⁻², respectively, which are superior to the reference device (43.3 cd A⁻¹, 15.4 lm W⁻¹).

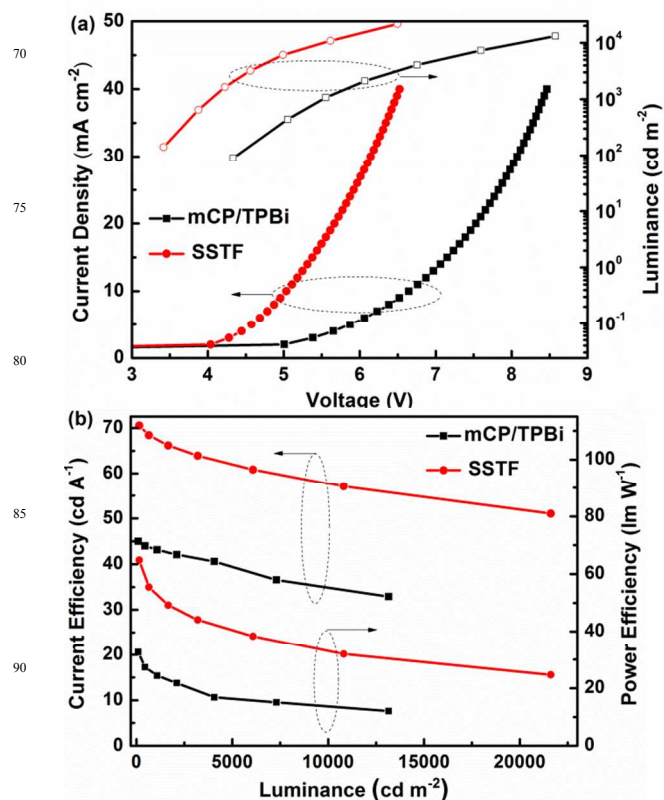


Fig 7. Current density-voltage-luminance (a), current and power efficiency-luminance (b) characteristics of device-mCP/TPBi, -SSTF.

Tandem White OLEDs

Tandem white phosphorescent OLEDs with two white EL units (emitting area: $3 \times 3 \text{ mm}^2$) were fabricated using Bphen: Li/Al/F₄-TCNQ/HAT-CN as an intermediate connector. Figure 8 shows the EL characteristics of tandem (two EL units) and conventional (single EL unit) WOLEDs. The detailed EL performance of tandem and conventional OLEDs are summarized in Table 1.

Table 1 Electroluminescence characteristics of the devices.

Device ^a	V ^b (V)	η c ^c (cd A ⁻¹)	η p ^c (lm W ⁻¹)	CIE ^d (x, y)
Single Unit	3.3, 3.9	70.9, 65	67.4, 52.3	(0.32, 0.46)
Tandem	7.2, 7.8	159.2, 152.3	69.4, 61.3	(0.37, 0.48)

^aSingle unit and tandem devices (Single unit & Tandem) size: 0.09 cm^2 .
^bDriving voltage at 100 cd m^{-2} and at 1000 cd m^{-2} . ^cEfficiencies in the order of 100 cd m^{-2} and 1000 cd m^{-2} . ^dCommission International de l'Eclairage coordinates measured at 5 mA cm^{-2} .

As seen from the J - V - L characteristics in Figure 8a, the operating voltage and luminance of the tandem device were almost doubled. The current and power efficiencies are shown in Figure 8b. The tandem device presents a current efficiency of 152.3 cd A^{-1} and a power efficiency of 61.3 lm W^{-1} at 1000 cd m^{-2} , which was much higher than that of conventional device (65 cd A^{-1} , 52.3 lm W^{-1}). Therefore, we have demonstrated that improved power efficiency can be achieved in the tandem OLEDs. It suggests that the intermediate connector of Bphen: Li/Al/F₄-TCNQ/HAT-CN exhibited excellent charge injection and transport characteristics without generating additional barrier in the tandem WOLEDs.

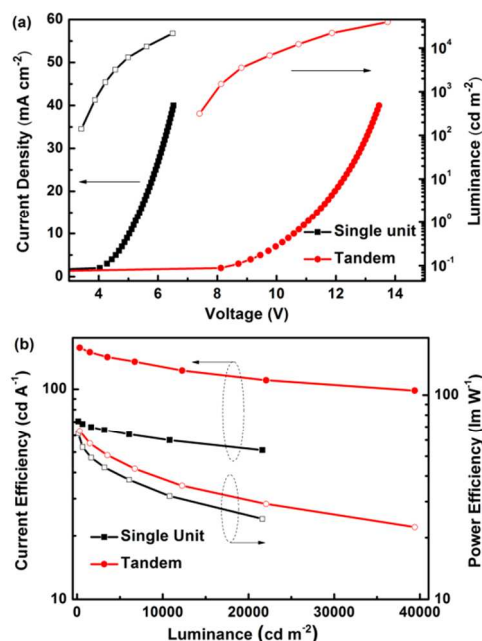


Fig 8. Current-voltage-luminance (a), current and power efficiency-luminance (b) characteristics of reference and tandem OLEDs.

$150 \times 150 \text{ mm}^2$ tandem White OLEDs

$(150 \times 150 \text{ mm}^2)$ WOLED lighting panel with- and without (W/O) diffuser film were fabricated. A series connection method was adopted for resolving the problem of power loss that exists in large-size OLED lighting panel. The whole lighting panel is divided into five light-emitting units, each unit includes a top electrode spaced apart from the top electrodes of other OLED units. However, each unit extends into electrical contact with the spaced apart bottom electrode of adjacent OLED device. And that the series connection of OLED devices is provided and current flows between the spaced apart top and bottom electrodes of each OLED device. Therefore, this method of fabricating large-size OLED panel can obviously reduce power loss due to series resistance. As seen from the J - L characteristics in Figure 9a, the luminance of the panel with diffuser film is about 60% higher than that of the panel without diffuser film. The inset is an emitting image of large-size $(150 \times 150 \text{ mm}^2)$ tandem WOLED lighting panel with diffuser film. Figure 9b shows the current and power efficiencies of the two lighting panels. The panel without any out-coupling technology demonstrates a maximum current efficiency of 144.9 cd A^{-1} and a maximum power efficiency of 33 lm W^{-1} , respectively. With a diffuser film covering, the maximum current and power efficiency is improved to be 231.8 cd A^{-1} and 52.9 lm W^{-1} , respectively.

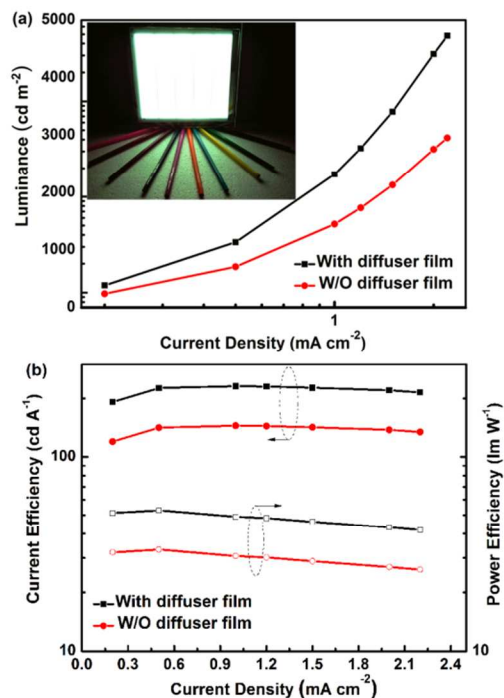


Fig 9. Luminance (a) and efficiencies (b) versus current density for the $150 \times 150 \text{ mm}^2$ tandem WOLED. Inset in (a): The image of large-area tandem WOLED.

Conclusions

In conclusion, a novel structure, utilizing Bphen: Li/Al/F₄-TCNQ/HAT-CN as an IC in tandem OLEDs has been proposed. The bilayer *p*-typed F₄-TCNQ/HAT-CN plays a critical effect in promotion of tandem WOLED performance owing to the formation of an efficient barrier gradient in the IC. Their roles of charge generation and separation need to be evidenced by evaluating the energy level via in-situ depositing and measuring techniques in the future. The tandem WOLED with a novel host material SSTF using the proposed IC structure achieved a maximum current efficiency of 70.5 cd A⁻¹ and power efficiency of 64.8 lm W⁻¹. Based on the bilayer *p*-type structure and novel host material, we fabricated a large-area white lighting prototype device with active area of 150 × 150 mm². In this device, a maximum efficiencies of 231.8 cdA⁻¹ and 52.9 lmW⁻¹ were achieved. Therefore, utilizing the series connection methods can effectively resolving the problem of power loss that exists in large-size OLED lighting panel. We believe that the concept of bilayer *p*-typed F₄-TCNQ/HAT-CN for the rational design of IC to realize tandem devices with unprecedented improvement in performance, in particular the large-area WOLEDs has great potentials for solid-state-lighting fabrication.

Supporting Information

Voltage-current density and current density-luminance characteristics of the hole-only device with MoO₃ in the different positions of IC. EL performances of green fluorescent tandem OLEDs with different intermediate connector. Proposed energy-level diagram of a white stacked OLED with two electrophosphorescent elements, the chemical structures of the materials used in this paper. EL performances of tandem white OLEDs with different intermediate connector.

Acknowledgements

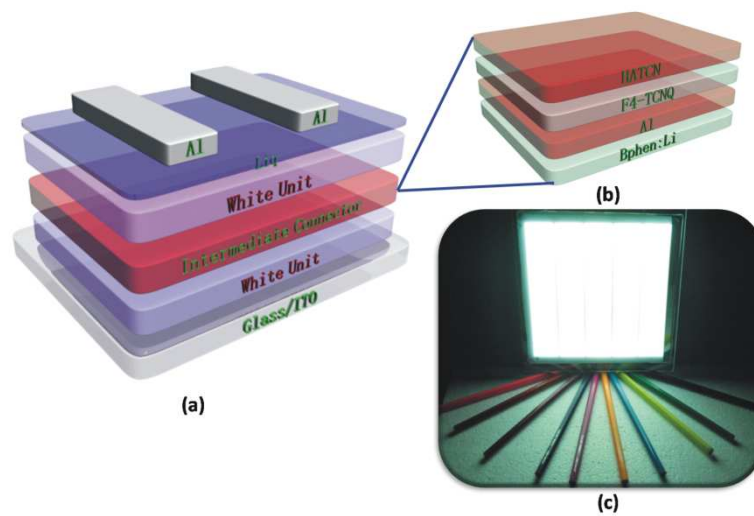
This work was supported by the Natural Science Foundation of China (Nos.21161160446, 61177016, 61036009, and 61307036). This is also a project funded by the Priority Academic Program Development of Jiangsu Higher Education Institutions (PAPD). By the Fund for Excellent Creative Research Teams of Jiangsu Higher Education Institutions, and by the Extracurricular Research Fund for University Students at Soochow University.

Notes and references

1. K. Sugi, T. Ono, D. Kato, T. Yonehara, T. S. Sawabe, I. Enomoto, Amemiya, *SID'12 Dig.*, 2012, **43**, 1548.
2. N. Ide, T. Komoda, J. Kido, *Proc. SPIE.*, 2006, **6333**, 63330.
3. X. Z. Zhu, Y. Y. Han, Y. Liu, K. Q. Ruan, M. F. Xu, Z. K. Wang, J. S. Jie, and L. S. Liao, *Org. Electron.*, 2013, **14**, 3348.
4. B.-W. D'Andrade, J. Esler, C. Lin, V. Adamovich, S. Xia, M.-S. Weaver, R. Kwong, J.-J. Brown, *Proc. SPIE.*, 2008, **143**, 70510.

5. S. Reineke, F. Lindner, G. Schwartz, N.-K. Walzer, B. Lüssem, K. Leo, *Nature*. 2009, **459**, 234.
6. C.-H. Gao, S.-D. Cai, W. Gu, D.-Y. Zhou, Z.-K. Wang, L.-S. Liao, *ACS Appl. Mater., Interfaces*. 2012, **4**, 5211.
7. M.-S. Kang, M.-K. Joo, J.-H. Lee, Y.-H. Ham, J.-B. Kim, K.-S. Moon, S. Son, *SID'11 Dig.*, 2011, **42**, 972.
8. T. Komoda, H. Tsuji, K. Yamae, K. Varutt, Y. Matsuhisa, N. Ide, *SID'11 Dig.*, 2011, **19**, 1056.
9. C.-L. Lin, M.-T. Lee, C.-W. Chen, C.-C. Lee, *SID'11 Dig.*, 2011, **19**, 1064.
10. T. Matsumoto, T. Nakada, J. Endo, K. Mori, N. Kawamura, A. Yokoi, J. Kido, *SID'03 Dig.*, 2003, **34**, 979.
11. M.-C. Gather, A. Köhnen, K. Meerholz, *Adv. Mater.*, 2011, **23**, 233.
12. J.-P. Yang, Y. Xiao, Y.-H. Deng, S. Duhm, N. Ueno, S.-T. Lee, Y.-Q. Li, J.-X. Tang, *Adv. Funct. Mater.*, 2012, **22**, 600.
13. J. Liu, S. Huang, X. Shi, X. Wu, J. Wang, G.-F. He, *J. Phys. Chem. C.*, 2013, **117**, 13887.
14. C.-C. Chang, J.-F. Chen, S.-W. Hwang, C.-H. Chen, *Appl. Phys. Lett.*, 2005, **87**, 253501.
15. K.-S. Yook, S.-O. Jeon, S.-Y. Min, J.-Y. Lee, H.-J. Yang, T. Noh, S.-K. Kang, T.-W. Lee, *Adv. Funct. Mater.*, 2010, **20**, 1797.
16. T.-W. Lee, T. Noh, B.-K. Choi, M.-S. Kim, D.-W. Shin, J. Kido, *Appl. Phys. Lett.*, 2008, **92**, 043301.
17. H. Kanno, R.-J. Holmes, Y. Sun, S.-K. Cohen, S.-R. Forrest, *Adv. Mater.*, 2006, **18**, 339.
18. L. Duan, T. Tsuboi, Y. Qiu, Y. Li, G. Zhang, *Opt. Express.*, 2012, **20**, 14564.
19. Y.-H. Chen, Q. Wang, J.-S. Chen, D.-G. Ma, D.-H. Yan, L.-X. Wang, *Org. Electron.*, 2012, **13**, 1121.
20. Y. Chen, J.-S. Chen, D.-G. Ma, D.-H. Yan, L.-X. Wang, F. Zhu, *Appl. Phys. Lett.*, 2011, **98**, 243309.
21. L.-S. Liao, K. Klubek, C. Tang, *Appl. Phys. Lett.*, 2004, **84**, 167.
22. M. Yokoyama, S.-H. Su, C.-C. Hou, C.-T. Wu, C.-H. Kung, *Jpn. J. Appl. Phys.*, 2011, **50**, 04DK06.
23. L.-S. Liao, K.-P. Klubek, *Appl. Phys. Lett.* 2008, **92**, 223311.
24. L.-S. Liao, W.-K. Slusarek, T.-K. Hatwar, M.-L. Ricks, D.-L. Comfort, *Adv. Mater.*, 2008, **20**, 324.
25. B.-J. Jung, K. Lee, J. Sun, A.-G. Andreou, H.-E. Katz, *Adv. Funct. Mater.*, 2010, **20**, 2930.
26. X.-B. Shi, M.-F. Xu, D.-Y. Zhou, Z.-K. Wang, L.-S. Liao, *Appl. Phys. Lett.* 2013, **102**, 233304.
27. P.-C. Kao, J.-H. Lin, J.-Y. Wang, C.-H. Yang, S.-H. Chen, *J. Appl. Phys.*, 2011, **109**, 094509.
28. H. Chen, Z.-Q. Jiang, C.-H. Gao, M.-F. Xu, S.-C. Dong, L.-S. Cui, S.-J. Ji, L.-S. Liao, *Chem. Eur. J.*, 2013, **19**, 11791.

Graphical abstract:



5